Experimental validation of Mueller matrix differential decomposition

Noé Ortega-Quijano,[1,2,*] Bicher Haj-Ibrahim,[1] Enric García-Caurel,[1] José Luis Arce-Diego,[2] and Razvigor Ossikovski[1]

[1]*LPICM, Ecole Polytechnique, CNRS, 91128 Palaiseau, France*
[2]*Applied Optical Techniques Group, Electronics Technology, Systems and Automation Engineering Department, University of Cantabria, Avenida de los Castros S/N, 39005 Santander, Cantabria, Spain*
**ortegan@unican.es*

Abstract: Mueller matrix differential decomposition is a novel method for retrieving the polarimetric properties of general depolarizing anisotropic media [N. Ortega-Quijano and J. L. Arce-Diego, Opt. Lett. 36, 1942 (2011), R. Ossikovski, Opt. Lett. 36, 2330 (2011)]. The method has been verified for Mueller matrices available in the literature. We experimentally validate the decomposition for five different experimental setups with different commutation properties and controlled optical parameters, comparing the differential decomposition with the forward and reverse polar decompositions. The results enable to verify the method and to highlight its advantages for certain experimental applications of high interest.

OCIS codes: (260.5430) Polarization; (260.2130) Ellipsometry and polarimetry; (120.5410) Polarimetry.

References and links

1. D. Goldstein, *Polarized Light* (Marcel Dekker, 2003).
2. R. Ossikovski, M. Anastasiadou, S. Ben Hatit, E. Garcia-Caurel, and A. De Martino, "Depolarizing Mueller matrices: how to decompose them," Phys. Status Solidi (A) **205**(4), 720–727 (2008).
3. S. R. Cloude, "Group theory and polarisation algebra," Optik (Stuttg.) **75**, 26–36 (1986).
4. S. R. Cloude, "Conditions for the physical realisability of matrix operators in polarimetry," Proc. SPIE **1166**, 177–185 (1989).
5. S. Y. Lu and R. A. Chipman, "Interpretation of Mueller matrices based on polar decomposition," J. Opt. Soc. Am. A **13**(5), 1106–1113 (1996).
6. J. J. Gil and E. Bernabeu, "Obtainment of the polarizing and retardation parameters of a non-depolarizing optical system from the polar decomposition of its Mueller matrix," Optik (Stuttg.) **76**, 67–71 (1987).
7. J. Morio and F. Goudail, "Influence of the order of diattenuator, retarder, and polarizer in polar decomposition of Mueller matrices," Opt. Lett. **29**(19), 2234–2236 (2004).
8. R. Ossikovski, A. De Martino, and S. Guyot, "Forward and reverse product decompositions of depolarizing Mueller matrices," Opt. Lett. **32**(6), 689–691 (2007).
9. M. Anastasiadou, S. Ben Hatit, R. Ossikovski, S. Guyot, and A. De Martino, "Experimental validation of the reverse polar decomposition of depolarizing Mueller matrices," J. Eur. Opt. Soc. Rapid Publ. **2**, 070181–070187 (2007).
10. R. Sridhar and R. Simon, "Normal form for Mueller matrices in polarization optics," J. Mod. Opt. **41**(10), 1903–1915 (1994).
11. R. Ossikovski, "Analysis of depolarizing Mueller matrices through a symmetric decomposition," J. Opt. Soc. Am. A **26**(5), 1109–1118 (2009).
12. C. Fallet, A. Pierangelo, R. Ossikovski, and A. De Martino, "Experimental validation of the symmetric decomposition of Mueller matrices," Opt. Express **18**(2), 831–842 (2010).
13. N. Ortega-Quijano, F. Fanjul-Vélez, I. Salas-García, and J. L. Arce-Diego, "Comparative study of optical activity in chiral biological media by polar decomposition and differential Mueller matrices analysis," Proc. SPIE **7906**, 790612 (2011).
14. N. Ortega-Quijano and J. L. Arce-Diego, "Mueller matrix differential decomposition," Opt. Lett. **36**(10), 1942–1944 (2011).
15. N. Ortega-Quijano and J. L. Arce-Diego, "Depolarizing differential Mueller matrices," Opt. Lett. **36**(13), 2429–2431 (2011).
16. N. Ortega-Quijano and J. L. Arce-Diego, "Mueller matrix differential decomposition for direction reversal: application to samples measured in reflection and backscattering," Opt. Express **19**(15), 14348–14353 (2011).
17. R. Ossikovski, "Differential matrix formalism for depolarizing anisotropic media," Opt. Lett. **36**(12), 2330–2332 (2011).

#156594 - $15.00 USD Received 14 Oct 2011; accepted 17 Nov 2011; published 4 Jan 2012

18. R. M. A. Azzam, "Propagation of partially polarized light through anisotropic media with or without depolarization: A differential 4x4 matrix calculus," J. Opt. Soc. Am. **68**(12), 1756–1767 (1978).
19. B. Laude-Boulesteix, A. De Martino, B. Drévillon, and L. Schwartz, "Mueller polarimetric imaging system with liquid crystals," Appl. Opt. **43**(14), 2824–2832 (2004).
20. E. Compain, S. Poirier, and B. Drevillon, "General and self-consistent method for the calibration of polarization modulators, polarimeters, and mueller-matrix ellipsometers," Appl. Opt. **38**(16), 3490–3502 (1999).
21. M. D. Waterworth, B. J. Tarte, A. J. Joblin, T. van Doorn, and H. E. Niesler, "Optical transmission properties of homogenised milk used as a phantom material in visible wavelength imaging," Australas. Phys. Eng. Sci. Med. **18**(1), 39–44 (1995).
22. M. I. Mishchenko, J. W. Hovenier, and L. D. Travis, *Light Scattering by Nonspherical Particles* (Academic, 2000).
23. R. R. Ansari, S. Böckle, and L. Rovati, "New optical scheme for a polarimetric-based glucose sensor," J. Biomed. Opt. **9**(1), 103–115 (2004).
24. S. Manhas, M. K. Swami, P. Buddhiwant, N. Ghosh, P. K. Gupta, and J. Singh, "Mueller matrix approach for determination of optical rotation in chiral turbid media in backscattering geometry," Opt. Express **14**(1), 190–202 (2006).
25. J. S. Maier, S. A. Walker, S. Fantini, M. A. Franceschini, and E. Gratton, "Possible correlation between blood glucose concentration and the reduced scattering coefficient of tissues in the near infrared," Opt. Lett. **19**(24), 2062–2064 (1994).
26. J. T. Bruulsema, J. E. Hayward, T. J. Farrell, M. S. Patterson, L. Heinemann, M. Berger, T. Koschinsky, J. Sandahl-Christiansen, H. Orskov, M. Essenpreis, G. Schmelzeisen-Redeker, and D. Böcker, "Correlation between blood glucose concentration in diabetics and noninvasively measured tissue optical scattering coefficient," Opt. Lett. **22**(3), 190–192 (1997).
27. A. N. Bashkatov, E. A. Genina, Y. P. Sinichkin, N. A. Lakodina, V. I. Kochubey, and V. V. Tuchin, "Estimation of glucose diffusion coefficient in scleral tissue," Proc. SPIE **4001**, 345–355 (2000).
28. N. Ghosh, M. F. G. Wood, and I. A. Vitkin, "Influence of the order of the constituent basis matrices on the Mueller matrix decomposition-derived polarization parameters in complex turbid media such as biological tissues," Opt. Commun. **283**(6), 1200–1208 (2010).

1. Introduction

During the past decades Mueller matrix polarimetry has been established as the main technique for optically characterizing polarization elements and media [1]. As a consequence of the growing interest in the applications of polarimetric characterization techniques, the analysis of experimental data is becoming increasingly relevant. Specifically, Mueller matrix decomposition techniques play a key role for appropriately studying and interpreting measurements.

A considerable number of Mueller matrix decompositions have been proposed so far [2]. Cloude decomposition is a sum-based decomposition that enables to describe the predominant polarizing optical behavior of a certain sample, as well as characterizing its depolarizing properties [3,4]. However, it is not able to separate all the optical effects and quantify them. Lu-Chipman polar decomposition [5] was proposed as the generalization of the polar decomposition for depolarizing media [6], and after that the method was extended for all the possible orderings of the basic optical elements [7–9]. It is currently the most widely used method among experimentalists for analyzing Mueller matrices, and it has enabled to obtain fruitful results in many applications. Other remarkable decompositions are the normal form decomposition [10] and the symmetric decomposition [11,12], being the latter comparatively easier to obtain and to interpret.

Despite the significant number of decompositions, there are still some difficulties that usually arise when experimentally measuring and analyzing samples. First of all, the order in which the effects take place in the sample may not be known a priori, and therefore the results are subjected to entail some errors [9]. And secondly, there are media in which the effects are produced in a distributed way, homogeneously, and not in a sequential fashion. In this case, product decompositions are prone to fail. It is not an obvious task to quantify and determine the experimental errors committed in this case for real situations.

Recently, a novel decomposition based on the differential formulation of the Mueller calculus has been presented [13–17]. The method was first proposed [14] as a natural consequence of the obtainment by means of Group theory of the complete set of differential Mueller matrices for describing general depolarizing anisotropic media [15]. Independently, the method was also proposed from the point of view of the physical interpretation of the

#156594 - $15.00 USD Received 14 Oct 2011; accepted 17 Nov 2011; published 4 Jan 2012

optical properties statistics by using the Minkowski antisymmetric and symmetric components [17]. In both cases, the differential Mueller calculus firstly proposed more than 30 years ago for non-depolarizing media [18] was extended for the general depolarizing case. Among the main advantages of the differential decomposition, the fact that it is specially suited for analyzing media with simultaneously occurring effects should be highlighted.

Mueller matrix differential decomposition has been proposed for both the forward and the backward direction. However, it has only been verified for a number of Mueller matrices of interest that can be found in the Optics literature. The aim of this work is to experimentally verify the method for several samples with controlled optical parameters and different characteristics in terms of number and ordering of optical effects.

2. Experimental

2.1 Polarimetric setup

The Mueller imaging polarimeter used in this work is schematically depicted in Fig. 1. The system can be divided into five main blocks: illumination system, polarization state generator, microscope system, polarization state analyzer, and detection system.

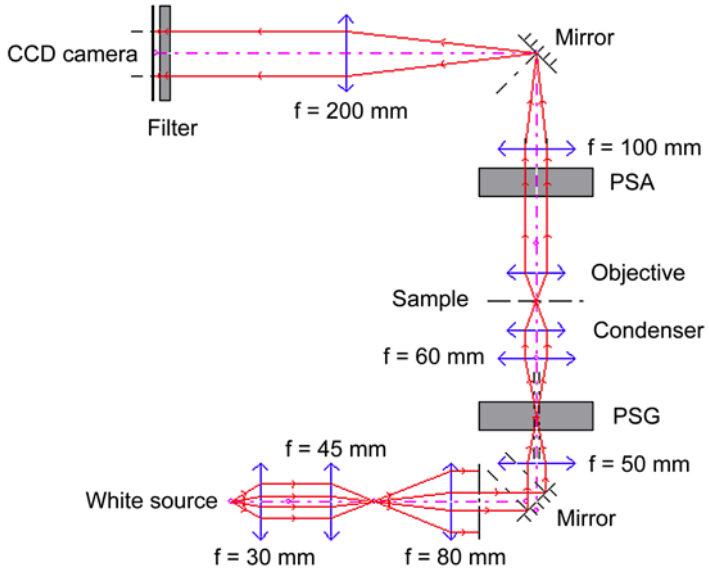

Fig. 1. Optical scheme of the microscopic Mueller imaging polarimeter in transmission.

The illumination system is formed by a halogen lamp (Olympus CLH-SC, 150W) with the output fiber bundle at the focus of an aspherical condenser (Thorlabs AC254, f = 30 mm), followed by a cold mirror, an achromatic lens (Thorlabs AC254, f = 45 mm), a diffuser and an achromatic collimator (Thorlabs AC254, f = 80 mm). This combination is telecentric in both the object and the image space. The system provides a total homogeneous illumination spot of about 2 cm diameter, which can be reduced by using a diaphragm. A beam splitter enables to take a reference in order to perform source normalization.

After the illumination system, an achromatic lens (Thorlabs AC254, f = 50 mm) focuses the incident light on the polarization state generator (PSG), which is composed of a linear polarizer (Melles Griot, 03 FPG 007) and two nematic liquid crystals variable retarders (Meadowlark LVR 300). At the output, an achromatic lens (Thorlabs AC254, f = 60 mm) collimates the spot. The design of the PSG design was performed following the optimized method developed in [19].

The microscope system is formed by the usual combination of condenser and objective. The objective used is a plan achromatic microscopic objective lens (Olympus SLMPlan 20x) with a numerical aperture of 0.35.

#156594 - $15.00 USD
Received 14 Oct 2011; accepted 17 Nov 2011; published 4 Jan 2012

The polarization state analyzer (PSA) is similar to the PSG, with a reverse disposition of the optical components, and following the same optimized design.

An ensemble formed by an achromatic lens (Thorlabs AC254, f = 100 mm) followed by a mirror and a second lens (Thorlabs AC254, f = 200 mm) projects the light spot in the detection system. Imaging is performed by a CCD camera (AVT Stingray F-080C, 786x432 pixels, 14 bits) with the aid of a zoom (Pentax TV lens 50 mm). An interference filter with a spectral bandwidth of 20 nm is placed before the detector in order to fix the detection wavelength, which in this case is fixed to 550 nm. The value of the dark current of the camera is taken before each measurement and is subtracted from the signal for each pixel. Five acquisitions were averaged for each measure in order to optimize the signal-to-noise ratio and subsequently increase the robustness and repeatability of the measurement. The calibration was performed using the Eigenvalue Calibration Method [20].

2.2 Samples

We have measured five different types of samples with different combinations of commutative and non-commutative optical effects that occur in a sequential and/or distributed way. They are shown in Fig. 2, where the arrow indicates the direction of light propagation.

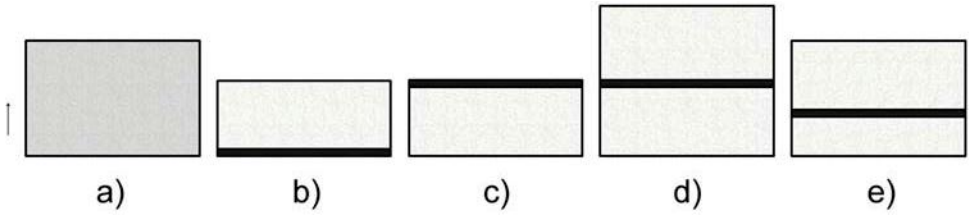

Fig. 2. Experimental samples scheme corresponding to a cuvette filled with a) glucose and milk dilution in distilled water, and milk dilution in distilled water with b) a linear polarizer at the bottom, c) a linear polarizer at the top, d) a linear polarizer symmetrically fixed inside the container, and e) a linear polarizer asymmetrically fixed inside the container. Dimensions are given in the text. The small arrow on the left indicates the light propagation direction.

2.2.1 Glucose and milk dilution in distilled water

The first sample (Fig. 2a) is an optically active turbid medium. A milk dilution in distilled water with different volume fractions was chosen as lipid-based scattering medium. Scattering in milk is produced fat globules surrounded by a lipid bilayer, which are typically 1 to 2 μm diameter, and also by casein proteins of about 0.15 μm diameter [21]. We used homogenized pasteurized milk with a fat content of 1.55%. The general form of the normalized Mueller matrix for such turbid medium is a diagonal depolarizer

$$\mathbf{M}_{\mathbf{turbid}} = \begin{bmatrix} 1 & 0 & 0 & 0 \\ 0 & d_l & 0 & 0 \\ 0 & 0 & d_l & 0 \\ 0 & 0 & 0 & d_c \end{bmatrix}, \qquad (1)$$

which is in agreement with the Mueller matrix observed in media with randomly located nearly spherical particles [22]. The d_l and d_c coefficients that characterize the diagonal depolarization shown by this kind of sample obviously vary according to the experimental parameters that determine the ensemble-averaged Mueller matrix measured in each case. Dextrogyre optical activity is obtained by adding different concentrations of glucose to the solution. The Mueller matrix for optical activity $\mathbf{M}_{\mathbf{oa}}$ is a rotation matrix. As long as the linear depolarization of the turbid medium is orientation-independent for linearly polarized light, the Mueller matrices of depolarization and optical activity remarkably commute:

#156594 - $15.00 USD Received 14 Oct 2011; accepted 17 Nov 2011; published 4 Jan 2012

$$\mathbf{M_{oa}M_{turbid}} = \mathbf{M_{turbid}M_{oa}} = \begin{bmatrix} 1 & 0 & 0 & 0 \\ 0 & d_l \cos 2\theta & d_l \sin 2\theta & 0 \\ 0 & -d_l \sin 2\theta & d_l \cos 2\theta & 0 \\ 0 & 0 & 0 & d_c \end{bmatrix}, \quad (2)$$

where θ is the rotation angle. The optical rotatory power of glucose at 550 nm is 61.36 °/(dm·g/mL) [23]. The solution was placed in a transparent glass cuvette with transversal dimensions of about 30x30 mm and a sample length of 10 mm.

2.2.2 Milk dilution with a linear polarizer at the bottom or at the top

The second and third samples are a combination a linear diattenuator and the turbid medium composed of milk and distilled water described above, which are placed sequentially with the diattenuator before (Fig. 2b) or after (Fig. 2c) the depolarizing medium. The diattenuator used in this work is a Polaroid film which was fixed into the cuvette with the transmission axis aligned with the horizontal axis of the detector. The length of the depolarizing medium in this case is 6.5 mm.

We would like to briefly discuss an important issue to be taken into account when analyzing these samples. The Mueller matrix of a horizontal diattenuator is

$$\mathbf{M_d}(p) = \begin{bmatrix} 1 & p & 0 & 0 \\ p & 1 & 0 & 0 \\ 0 & 0 & \left(1-p^2\right)^{1/2} & 0 \\ 0 & 0 & 0 & \left(1-p^2\right)^{1/2} \end{bmatrix}, \quad (3)$$

where p is the diattenuation coefficient. The four eigenvalues of $\mathbf{M_d}(p)$ are $\lambda^1_{\mathbf{M_d}(p)} = 1+p$, $\lambda^2_{\mathbf{M_d}(p)} = 1-p$, and $\lambda^3_{\mathbf{M_d}(p)} = \lambda^4_{\mathbf{M_d}(p)} = \left(1-p^2\right)^{1/2}$. A perfect diattenuator corresponds to the limit $\mathbf{M_d^{ideal}}(p) = \lim_{p\to 1}\left\lfloor \mathbf{M_d}(p) \right\rfloor$. In that case, the Mueller matrix of the diattenuator is singular, with a single non-zero eigenvalue. An important consequence is that the differential Mueller matrix cannot be calculated for perfect diattenuators, as long as the matrix logarithm is not defined for singular matrices. However, perfect diattenuators are only a theoretical idealization, but in practice perfect diattenuators do not exist. Even for values of the diattenuation coefficient extremely close to 1, the Mueller matrix still has four non-zero eigenvalues, and therefore the calculation of the matrix logarithm is always possible for this kind of devices. In addition, the presence of noise in the measurements produces the same effect. In this latter situation, special attention should be paid to the physical realizability of the measured matrix (see Section 2.3). As a result, we can conclude that, from a phenomenological point of view, in practice we will always be applying the method to non-singular Mueller matrices.

The Mueller matrices of depolarization and linear diattenuation do not commute. The Mueller matrix for the diattenuator followed by the depolarizer is

$$\mathbf{M_{turbid}M_d}(p) = \begin{bmatrix} 1 & p & 0 & 0 \\ d_l p & d_l & 0 & 0 \\ 0 & 0 & d_l\left(1-p^2\right)^{1/2} & 0 \\ 0 & 0 & 0 & d_c\left(1-p^2\right)^{1/2} \end{bmatrix}, \quad (4)$$

while the matrix for the reverse order (depolarizer followed by the diattenuator) is

#156594 - $15.00 USD Received 14 Oct 2011; accepted 17 Nov 2011; published 4 Jan 2012

$$\mathbf{M_d}(p)\mathbf{M_{turbid}} = \begin{bmatrix} 1 & d_l p & 0 & 0 \\ p & d_l & 0 & 0 \\ 0 & 0 & d_l\left(1-p^2\right)^{1/2} & 0 \\ 0 & 0 & 0 & d_c\left(1-p^2\right)^{1/2} \end{bmatrix}. \quad (5)$$

So, in fact, it is readily verified that the Mueller matrix corresponding to one of the possible ordering of the elements is just the transpose of the other one. This fact is relevant for the assessment of the experimental data presented in Section 3.

2.2.3 Milk dilution with a linear polarizer inside the container

The last two samples are similar to the second and third samples, with the relevant difference that the polarizer is placed inside the turbid medium. The Mueller matrix in this case is:

$$\mathbf{M_{turbid2}}\mathbf{M_d}(p)\mathbf{M_{turbid1}} = \begin{bmatrix} 1 & d_{l1} p & 0 & 0 \\ d_{l2} p & d_{l1} d_{l2} & 0 & 0 \\ 0 & 0 & d_{l1} d_{l2}\left(1-p^2\right)^{1/2} & 0 \\ 0 & 0 & 0 & d_{c1} d_{c2}\left(1-p^2\right)^{1/2} \end{bmatrix}. \quad (6)$$

In the fourth sample (Fig. 2d) the linear polarizer is symmetrically fixed inside the container (which in this case has a total length of 13 mm) so it can be considered that $d_{l1} = d_{l2} = d_l$. When macroscopically measured, such type of sample constitutes an appropriate model of a medium with distributed simultaneous optical properties. The last sample (Fig. 2e) has the linear polarizer asymmetrically fixed inside a glass container of 10 mm, with a distance of 3.5 mm to the bottom and 6.5 mm to the top, so for this situation $d_{l1} \neq d_{l2}$.

2.3 Method

The microscopic Mueller imaging polarimeter described above gives sixteen images corresponding to each Mueller matrix coefficient. Each image is 800x600 pixels, from which the active area radius is 350 pixels. For this study we select a fixed 40x40 pixels window in the center of the image. All the images are normalized to the first Mueller matrix element.

The first step is filtering the measured matrix in order to correct residual experimental errors and ensure that the physical realizability condition of the measured Mueller matrix is fulfilled [4]. The filtering procedure requires calculating the covariance matrix $\mathbf{C}$ from the Mueller matrix $\mathbf{M}$ for each pixel

$$\mathbf{C} = \sum_{i,j=1}^{4} \mathbf{M_{ij}}\left(\boldsymbol{\sigma}_\mathbf{i} \otimes \boldsymbol{\sigma}_\mathbf{j}^*\right), \quad (7)$$

where * denotes the complex conjugate and $\otimes$ is the Kronecker product that enables to obtain the sixteen Dirac matrices from the Pauli spin matrices $\boldsymbol{\sigma}_\mathbf{i}$. The covariance matrix is further diagonalized by a conventional eigen decomposition so that $\mathbf{C} = \mathbf{V_C}\mathbf{D_C}\mathbf{V_C^{-1}}$, where $\mathbf{D_C}$ is a diagonal matrix with the eigenvalues of $\mathbf{C}$ (we will denote them λ_C) and $\mathbf{V_C}$ contains its eigenvectors column-wise. Matrix filtering consists on fixing any negative eigenvalue to zero, and subsequently obtaining the filtered Mueller matrix by inverting Eq. (7).

Once the matrix has been filtered, it is decomposed by two different methods: the polar decomposition [5–7] and the differential decomposition [14–17]. Regarding polar

#156594 - $15.00 USD Received 14 Oct 2011; accepted 17 Nov 2011; published 4 Jan 2012

decomposition, we will use two specific decompositions out of the six possible products, namely the forward decomposition in its most common order

$$\mathbf{M} = \mathbf{M}_{\Delta}^{\mathbf{f}} \mathbf{M}_{\mathbf{R}}^{\mathbf{f}} \mathbf{M}_{\mathbf{D}}^{\mathbf{f}}, \tag{8}$$

which is usually called Lu-Chipman polar decomposition with reference to the authors that first proposed it, and the reverse decomposition in its form

$$\mathbf{M} = \mathbf{M}_{\mathbf{R}}^{\mathbf{r}} \mathbf{M}_{\mathbf{D}}^{\mathbf{r}} \mathbf{M}_{\Delta}^{\mathbf{r}}. \tag{9}$$

The differential decomposition is performed by obtaining the accumulated differential Mueller matrix from the matrix logarithm of the macroscopic Mueller matrix

$$\bar{\mathbf{m}} = \mathrm{logm}(\mathbf{M}), \tag{10}$$

which can be easily calculated by the eigen analysis of $\mathbf{M}$, and further decomposing it into the 16 differential parameters that characterize general depolarizing anisotropic media [14,17].

In this work we have used three different parameters to characterize the optical properties of the measured samples: optical rotation, diattenuation coefficient, and entropy. These parameters are calculated for each pixel, and the results are statistically analyzed to obtain the mean value and the standard deviation in the observation window. Optical rotation can be calculated from the retardance component of any polar decomposition as

$$\Psi_{lc} = \frac{1}{2} \mathrm{atan}\left[\frac{\mathbf{M}_{\mathbf{R}}(3,2) - \mathbf{M}_{\mathbf{R}}(2,3)}{\mathbf{M}_{\mathbf{R}}(2,2) + \mathbf{M}_{\mathbf{R}}(3,3)} \right], \tag{11}$$

while for differential decomposition the optical rotation is simply given by

$$\Psi_{dd} = -\bar{\eta}_v / 2, \tag{12}$$

where the minus sign arises from the sign convention adopted in the definition of the general differential Mueller matrix. Regarding the diattenuation coefficient, it can be obtained from the diattenuation component of polar decomposition

$$D_{lc} = \frac{1}{\mathbf{M}_{\mathbf{D}}(1,1)} \left[\mathbf{M}_{\mathbf{D}}(1,2)^2 + \mathbf{M}_{\mathbf{D}}(1,3)^2 + \mathbf{M}_{\mathbf{D}}(1,4)^2 \right]^{1/2}. \tag{13}$$

In the case of differential decomposition, the diattenuation coefficient is given as a function of the elementary optical properties of the sample by

$$D_{dd} = \tanh\left[\left(\bar{\kappa}_q^{\,2} + \bar{\kappa}_u^{\,2} + \bar{\kappa}_v^{\,2} \right)^{1/2} \right], \tag{14}$$

where $\bar{\kappa}_q$, $\bar{\kappa}_u$ and $\bar{\kappa}_v$ are the accumulated differential parameters for linear x-y, linear ± 45° and circular dichroism, respectively [14]. It should be highlighted that the accumulated differential parameters diverge for an ideal depolarizer, while the diattenuation coefficient defined in Eq. (14) always takes values below 1, as expected from the definition of this metric. This expression for calculating the diattenuation coefficient can be easily obtained from the solution of the differential matrix and Mueller matrix eigenvalue equations [18] in a similar way as it was performed for the differential Jones matrix of a general diattenuator [5].

Finally, depolarization is quantified by the entropy-like depolarization metric H [3], defined from the eigenvalues of the Cloude coherency matrix as

$$H = \sum_{i=1}^{4} x_i \log_4 x_i, \quad x_i = \lambda_{Ci} \Big/ \sum_{j=1}^{4} \lambda_{Ci}. \tag{15}$$

#156594 - $15.00 USD Received 14 Oct 2011; accepted 17 Nov 2011; published 4 Jan 2012

3. Results

3.1 Validation for commutative distributed effects

The first set of measurements was performed on optically active turbid samples as already described in Section 2.2. Glucose concentrations of 0M, 0.62M, 1.15M, 1.62M and 2.03M were measured with several milk concentrations for each of them, in order to have entropy values from 0 (no depolarization) to nearly 1 (complete depolarization). First of all, the scattering solution without glucose was measured for control purposes. Figure 3 shows the mean values and standard deviations obtained for the 40x40 pixels window as described in Section 2.3. The calculated optical rotation is nearly zero for all cases. The standard deviation of the measurement (which coincides for the three decompositions) increases as depolarization becomes stronger, but the stability of the average optical rotation values confirms the quality of the measurements. It can be observed that the results all the decompositions overlap, as expected for commutative optical effects, as long as the order assumption performed in polar decomposition does not affect in this case.

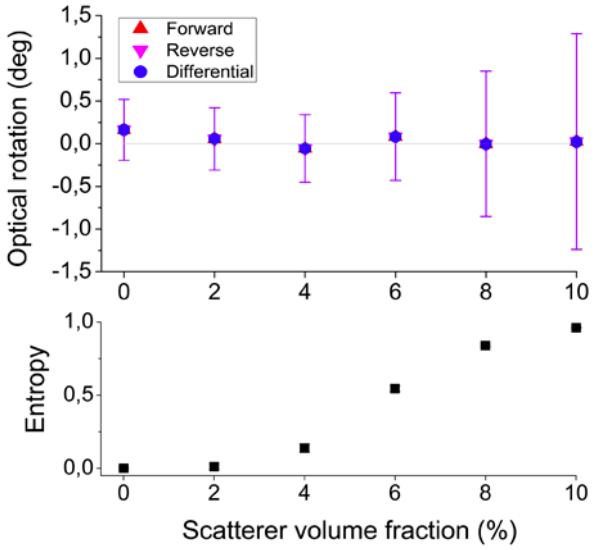

Fig. 3. Optical rotation as a function of the scatterer concentration for a milk dilution in distilled water without glucose. The theoretical value (zero) is depicted as a reference. The inset at the bottom shows the Cloude entropy for each value of milk volume fraction. Error bars represent the standard deviation, which overlaps for the three decompositions.

The results for glucose concentrations of 1.15M are presented in Fig. 4 (similar results were obtained for the rest of concentrations and are not shown here for the sake of conciseness). The calculated optical rotation for the cuvette length is 1.47 degrees (it has been depicted with a grey line). The experimental results are in very good agreement with the expected value. A remarkable increase in the standard deviation is observed in the same way as above. It is interesting to note that the observed optical rotation slightly increases for higher milk concentrations. This effect is due to the average path length increase caused by multiple scattering, and has already been observed in other experimental measurements [24]. The results obtained by the three decompositions coincide again, which enables to validate the experimental accuracy of Mueller matrix differential decomposition.

The previous results show the optical rotation values for a fixed glucose concentration and increasing milk volume fraction. However, there is a remarkable effect that can be observed when the glucose concentration increases for a fixed milk volume fraction. Scattering depends on both the size parameter and the optical contrast between the scattering particles and the background medium. Provided that glucose refractive index at 550 nm is 1.48, the refractive

#156594 - $15.00 USD
Received 14 Oct 2011; accepted 17 Nov 2011; published 4 Jan 2012

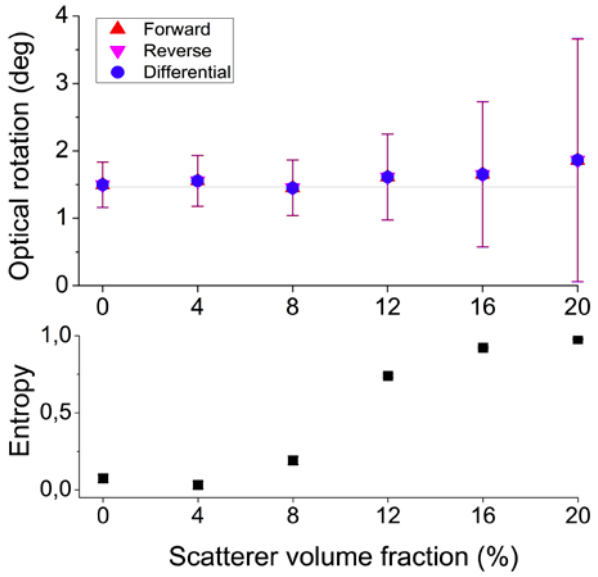

Fig. 4. Optical rotation as a function of the scatterer concentration for a milk dilution in distilled water with a glucose molar concentration of 1.15M. The theoretical value (zero) is depicted as a reference. The inset at the bottom shows the Cloude entropy for each value of milk volume fraction. Error bars represent the standard deviation, which overlaps for the three decompositions.

index of the glucose dilution in distilled water $n_{dilution}$ can be expressed as a function of the glucose volume fraction f_{glucose} by the equation $n_{dilution} = 1.33\left(1 - f_{\text{glucose}}\right) + 1.48 f_{\text{glucose}}$. On the other hand, a typical value of the lipid globules refractive index is about 1.45. Therefore, an increase in glucose concentration can significantly reduce the optical contrast between the scattering particles and the background medium, with a subsequent reduction in the scattering coefficient of the sample. This effect has been previously observed and proposed for non-invasively determining glucose concentration in blood [25,26] and in the eye sclera [27]. We have experimentally observed such type of variations in the depolarizing properties of our samples. Figure 5 shows the reduction of the Cloude entropy as a function of the glucose

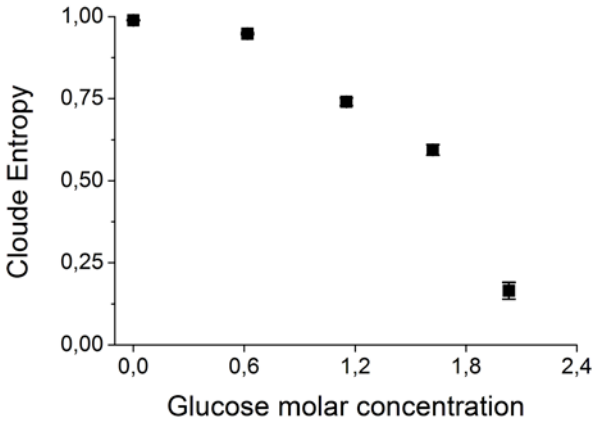

Fig. 5. Variation of the Cloude entropy as a function of the glucose concentration for a milk volume fraction of 12%.

#156594 - $15.00 USD
Received 14 Oct 2011; accepted 17 Nov 2011; published 4 Jan 2012

concentrations for a fixed milk volume fraction, which in this case is 12%. It can be observed that the entropy diminishes from 1 to 0.16 for the considered glucose concentrations, which highlights the relevance of this effect as well as its influence on the measurements.

3.2 Comparison for non-commutative sequential effects

The results obtained by polar decomposition depend on the choice of the most appropriate sub-type of decomposition for a certain measurement. The accuracy of the results is obviously better if the assumption about the order in which the optical effects take place corresponds to the real physical conditions of the experiment. However, the choice becomes difficult if no aprioristic information about the sample is known. In this case, the non-commutativity of matrix products can lead to erroneous results [7–9].

The order-dependence of polar decomposition is evident for the milk dilution with a linear polarizer at the bottom and at the top (second and third samples described in Section 2.2). The Mueller matrix for such samples has been presented in Eqs. (4) and (5). The first step in polar decomposition is calculating the diattenuator matrix. Both the first row and the first column of the diattenuator matrix are directly obtained from the measured Mueller matrix. The forward polar decomposition takes the diattenuation vector (the first row of the Mueller matrix under analysis) while the reverse polar decomposition takes the polarizance vector (the first column of the Mueller matrix) [8]. The diattenuation coefficient can be subsequently calculated by the expression given in Eq. (13) from the first column of the Mueller matrix of the diattenuator obtained from the previous step [8]. As a result, it can be readily verified that the calculated diattenuation coefficient for the second and third samples is p as expected when the order assumption is correct, while it is $d_l p$ when the order assumption is wrong. Consequently, for nearly perfect polarizers, the calculated diattenuation coefficient is roughly the linear diagonal depolarization coefficient d_l when using the inappropriate polar decomposition.

Several measurements have been performed on samples with sequential effects in order to observe the order-dependence of polar decomposition and compare it with the results obtained by the differential decomposition for such kind of samples. The first sample is a diattenuator followed by a depolarizer (Fig. 2b). The measured diattenuation coefficient for the Polaroid film alone is 0.9992. Figure 6 shows the diattenuation coefficient obtained for several milk volume fractions, as well as the Cloude entropy of each sample. The diattenuation coefficient calculated by the differential decomposition and the forward polar decomposition is roughly one for all cases, as expected. However, it can be observed that the reverse polar

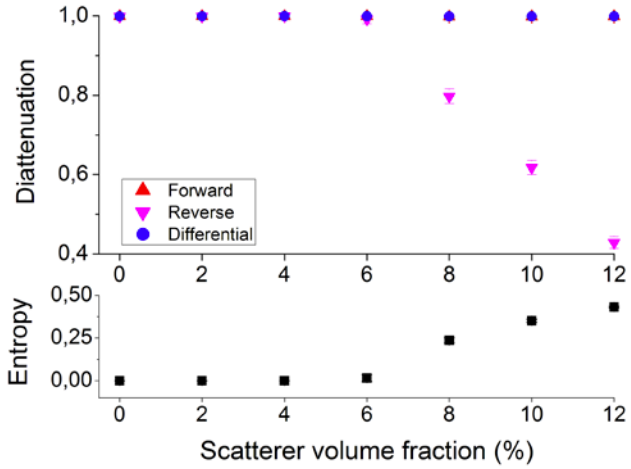

Fig. 6. Diattenuation coefficient as a function of the milk volume fraction for the configuration diattenuator-depolarizer (Fig. 2b). The inset at the bottom shows the Cloude entropy for each value of milk volume fraction.

#156594 - $15.00 USD
Received 14 Oct 2011; accepted 17 Nov 2011; published 4 Jan 2012

decomposition is assuming the wrong order, which provokes a stronger error in the results for increasing depolarization. We should recall that the forward and reverse polar decompositions obviously give the same result when the entropy is small (in that situation there is only an optical effect, as long as no depolarization is produced in the sample).

A similar situation is observed for the opposite configuration: a depolarizer followed by a diattenuator (Fig. 2c). In that case, the reverse polar decomposition is assuming the correct order, while the forward decomposition fails. As a result, the forward decomposition gives wrong diattenuation coefficients, with an error trend that is similar to the one observed for the previous experimental configuration. The results can be observed in Fig. 7. In fact, the calculated values obtained for the forward and reverse experimental setup are nearly the same (reversing the correct and wrong order for each case), which corroborates the accuracy of the measurements.

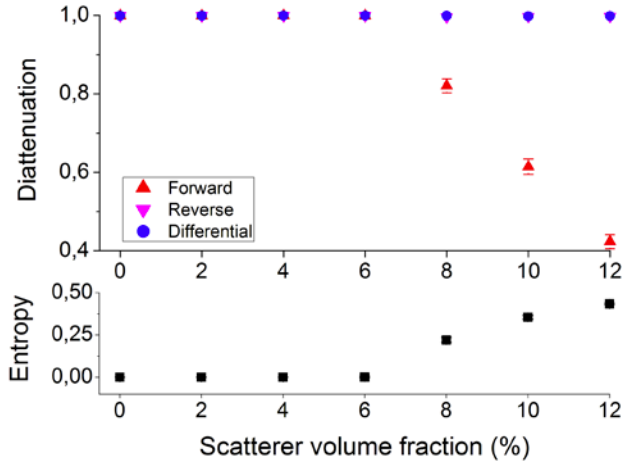

Fig. 7. Diattenuation coefficient as a function of the milk volume fraction for the configuration depolarizer-diattenuator (Fig. 2c). The inset at the bottom shows the Cloude entropy for each value of milk volume fraction.

3.3 Comparison for non-commutative distributed-like effects

Apart from the choice of the order, there is another problem that usually arises: there are many samples in which the optical effects take place simultaneously, in a distributed way. Biological tissues constitute a relevant example of such kind of media. In that case, the assumption of sequential and discrete optical effects is arbitrary and does not correspond to the real physical characteristics of the sample. Even if the errors can remain moderate for certain conditions [28], using a family of decompositions that are based on non-commutative matrix products constitutes a not so suitable methodology. For such kind of experimental samples, the differential Mueller matrix decomposition constitutes a more appropriate approach, as long as it is order-independent and it appropriately models simultaneous optical effects at the microscopic level.

In order to verify the differential decomposition for such kind of media, we have measured the milk dilution with the polarizer in the middle (Fig. 2d) described in Section 2.2, as long as it mimics a medium with non-commutative distributed effects. The fact that this sample has controlled optical properties is determinant for the verification of our method, as a necessary step before applying it for analyzing media of increasing complexity.

For this sample, both the forward and reverse polar decompositions give erroneous results for the diattenuation coefficient. From Eq. (6) it can be easily seen that a diattenuation coefficient of $d_l p$ is obtained by both polar decompositions when the Polaroid is symmetrically placed inside the container. The experimental results are shown in Fig. 8.

#156594 - $15.00 USD
Received 14 Oct 2011; accepted 17 Nov 2011; published 4 Jan 2012

Effectively, it can be observed that the diattenuation coefficient calculated by polar decomposition begins to fail as soon as the depolarization shown by the sample becomes noticeable. The values calculated by the forward and reverse decompositions are roughly the same, as predicted (the slight difference between them is likely due to small differences in the turbid medium length before and after the polarizer). However, the differential decomposition shows a robust behavior in the determination of the diattenuation coefficient for all cases. In effect, it manages to decouple the optical effects and successfully characterizes the diattenuation properties of the sample.

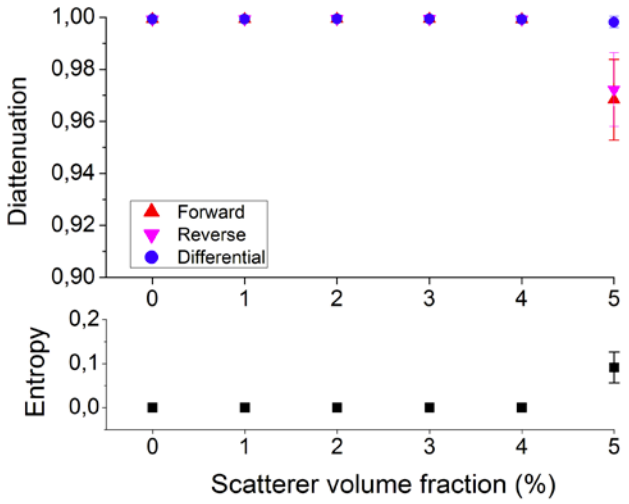

Fig. 8. Diattenuation coefficient as a function of the milk volume fraction for the polarizer symmetrically placed inside the turbid medium (Fig. 2d).

It is important to note that the maximum depolarization observed in the previous measurements corresponds to a Cloude entropy of 0.09, as can be observed in Fig. 8. This weak depolarization effect does not enable to observe a stronger decrease in the diattenuation coefficients calculated by both types of polar decompositions. This constraint is due to experimental limitations of the polarimeter for measuring this sample, as long as the high extinction forced to reach the limit of the acquisition time. The last sample considered in this work enables to better observe the effect of the sample depolarization in the obtained coefficients. The milk dilution with the polarizer asymmetrically placed inside the container (Fig. 2e) presents interesting characteristics for our study. In this case, each type of polar decomposition fails in a different way. From Eq. (6), and for this sample, both the forward and reverse polar decompositions give erroneous results for the diattenuation coefficient. Following the same considerations as above, it can be readily verified that the forward decomposition estimates a diattenuation coefficient of $d_{l1}p$, while the reverse decomposition calculates a diattenuation coefficient of $d_{l2}p$. The measurements for this sample are presented in Fig. 9. The maximum Cloude entropy observed in this case is 0.306. The errors committed by polar decompositions are in agreement with the expected behavior. In depolarizing media, the d_l coefficient is directly proportional to the length of the sample. Therefore, for the experimental configuration shown in Fig. 2e and according to the order established in Eq. (6), d_{l1} is smaller than d_{l2}, and therefore the error committed in this case should be smaller for the forward decomposition, as confirmed by the experimental results. The behavior of the differential decomposition is the same as in all the previous samples considered above, giving a diattenuation coefficient of roughly 1 for all the measurements.

#156594 - $15.00 USD Received 14 Oct 2011; accepted 17 Nov 2011; published 4 Jan 2012

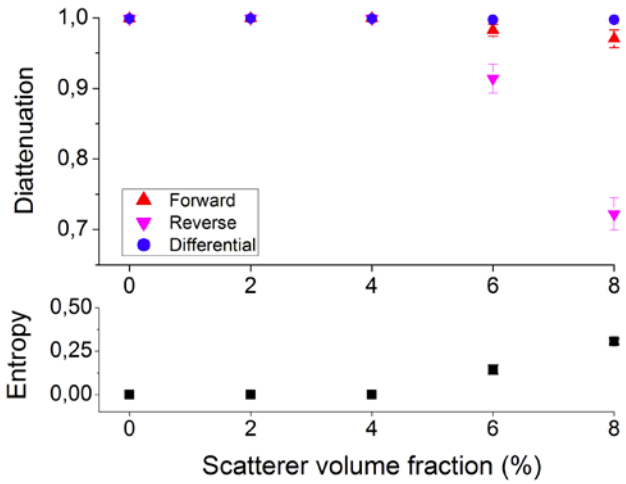

Fig. 9. Diattenuation coefficient as a function of the milk volume fraction for the polarizer asymmetrically placed inside the turbid medium (Fig. 2e).

4. Conclusions

The experimental verification of Mueller matrix differential decomposition has been presented for the first time. The validation of this method has been demonstrated for several types of media measured in transmission. Samples with commutative distributed effects, non-commutative sequential effects, and non-commutative distributed-like ones have been measured and analyzed using the forward and reverse polar decompositions and the differential decomposition. The results enable to assess the validity of the differential decomposition for appropriately analyzing the experimental data obtained by imaging Mueller polarimeters. The order-independence of the differential decomposition and its suitability for studying media with simultaneous optical effects makes it a technique with a high potential for many applications. In particular, the analysis of biological tissues polarimetric images seems one of the most interesting applications of this novel method.

Acknowledgments

This work has been partially funded by the San Cándido Foundation, Santander (Spain). Part of this work has been supported by a Predoctoral Grant of the University of Cantabria. Bicher Haj-Ibrahim gratefully recognizes partial funding within the ANR *ScatteroMueller* contract.

#156594 - $15.00 USD Received 14 Oct 2011; accepted 17 Nov 2011; published 4 Jan 2012